

https://doi.org/10.1070/QEL17268

Features of multilayer mirror application for focusing and collimating X-rays from inverse Compton scattering sources

M.M. Barysheva, I.V. Malyshev, V.N. Polkovnikov, N.N. Salashchenko, M.V. Svechnikov, N.I. Chkhalo

Abstract. **We have analysed the use of X-ray interference multilayer mirrors as the elements of a focusing scheme for a compact source based on inverse Compton scattering. An algorithm is proposed for selecting mirror parameters, which takes into account the properties of the radiation source. The dependence of wavelength on the viewing angle and the energy line broadening for a fixed viewing angle are found to be the main limitations in the use of multilayer mirrors. Efficient radiation collection calls for the application of broadband mirrors. It is shown that the efficiency of multilayer mirrors in a Kirkpatrick–Baez X-ray focusing setup exceeds that of total external reflection mirrors by an order of magnitude, and that stack multilayer mirrors offer a small advantage over the periodic ones. The overall efficiency of source radiation collection in the photon energy range ΔE = 10–12 keV amounts to 12% for the two-mirror Kirkpatrick–Baez setup. For a spectral region with a bandwidth $\Delta E/E$ = 3%, the efficiency ranges up to 69%.**

Keywords: *compact X-ray source, inverse Compton effect, multilayer mirrors, broadband mirrors, stack mirrors, Kirkpatrick–Baez setup.*

1. Introduction

High-power compact hard X-ray sources are used in research and medical laboratories. Among the disadvantages of classical X-ray tube sources are low brightness and wavelength tuning limitations associated with a broad bremsstrahlung spectrum and with individual intense characteristic lines. Synchrotron sources, which provide the possibility of wavelength tuning and high brightness, cannot be applied in laboratory conditions. Furthermore, the short-wavelength bound of the photon spectrum is limited to energies of 300–500 keV even for the most modern synchrotrons that use last-generation undulators, while a broad class of problems invites high-intensity high-energy X-ray beams [1]. Recent years has seen numerous papers concerned with the development of a compact laboratory X-ray source harnessing the effect of inverse Compton scattering [2–5].

Since the cross sections for the Thomson scattering of laser radiation by relativistic electrons, $\sigma_T = (8/3) \times \pi r_e^2 = 0.665 \times 10^{-24}$ cm^2, are extremely low, it was previously believed that this effect has no practical application. However, the efficiency of this X-ray source became higher with the advent of high-power femtosecond lasers and special-purpose accelerators that generate high-repetition-rate electron bunches focusable to an area several micrometres in size. The placement of laser beam–electron interaction region into a power enhancement laser cavity, which increased the effective average laser power in the interaction region by several orders of magnitude, entailed an even greater growth of generated radiation power up to values of practical interest [5].

X-ray sources based on inverse Compton effect are developed for biomedical applications [6, 7]. In particular, compact sources may be used in the development of phase-contrast imaging for diagnosing cancer and cardiac diseases, which were previously tested with synchrotron sources. Due to a continuous radiation frequency tuning, they may be employed in X-ray absorption spectroscopy, diffraction and several other tasks. For instance, Hornberger et al. [5] have recently described a compact X-ray source with a tunable operating wavelength corresponding to an energy range of 15–35 keV, a bandwidth $\Delta E/E \approx 3\%–5\%$, and an intensity of $\sim 3 \times 10^{10}$ photon s^{-1}. In this case, the source size was ~100 μm. Also reported in Ref. [5] was the development of a next-generation device with a smaller source size (~80 μm), a broader wavelength range (8–42 keV), and an order of magnitude higher X-ray flux ($\sim 3 \times 10^{11}$ photon s^{-1}).

An efficient practical use of such a source calls, in particular, for an optimal choice of the X-ray optical elements that collect, collimate, or focus the X-ray beam. Owing to a relatively large angular divergence of the radiation, small-aperture refractive lenses [8] turn out to be inefficient. These problems may be optimally solved with the use of single or crossed mirrors (the Kirkpatrick–Baez setup [9]). Since the source is quite new and still little used in practice, it is necessary to take into account its properties in the development of specular optics. This paper analyses the use of X-ray mirrors of various types as reflecting and focusing elements of the optical setup of the source. Mirrors based on the total external reflection, periodic multilayer mirrors, and broadband stack mirrors are considered. Our analysis is carried out by the example of a source with a maximum photon energy of 12 keV, which is being developed for materials science research.

M.M. Barysheva Institute for Physics of Microstructures, Russian Academy of Sciences, ul. Akademicheskaya 7, 603087 Afonino, Kstovskii raion, Nizhny Novgotod region, Russia; Lobachevsky State University of Nizhny Novgorod, prosp. Gagarina 23, 603950 Nizhny Novgorod, Russia; e-mail: mmbarysheva@ipmras.ru;
I.V. Malyshev, V.N. Polkovnikov, N.N. Salashchenko, M.V. Svechnikov, N.I. Chkhalo Institute for Physics of Microstructures, Russian Academy of Sciences, ul. Akademicheskaya 7, 603087 Afonino, Kstovskii raion, Nizhny Novgotod region, Russia

Received 4 February 2020
Kvantovaya Elektronika **50** (4) 401–407 (2020)
Translated by E.N. Ragozin

2. Spectral properties of a source based on inverse Compton effect

Let us consider the properties of the emission spectrum of a source based on inverse Compton scattering that affect the choice of mirrors. The expression for the energy E of photons scattered by an angle θ in the head-on collision with a relativistic electron may be written as

$$E(\theta) = \frac{4E_L\gamma^2}{1+\gamma^2\theta^2}, \quad (1)$$

where E_L is the energy of a laser photon; $\gamma = E_e/E_0$ is the relativistic factor; E_e is the electron energy; and $E_0 = 0.511$ MeV is the electron rest energy. Formula (1) is written under the assumptions that $E_e \gg E_0$, $E_L \ll E_0$, and $\theta \ll 1$. According to expression (1), to every photon scattering angle there corresponds an X-ray photon wavelength (energy) of its own. In view of relation $E_L = hc/\lambda_0$ (λ_0 is the wavelength of laser radiation), the maximum energy is defined as

$$E_{max} = \frac{4hc}{\lambda_0}\gamma^2. \quad (2)$$

Relation (1) between the scattering angle θ and the photon energy E may also be represented as a function of E_{max}:

$$E(\theta) = \frac{E_{max}}{1+\frac{\lambda_0}{4hc}E_{max}\theta^2}, \quad (3)$$

or

$$\theta^2(E) = \frac{4hc}{\lambda_0}\left(\frac{1}{E}-\frac{1}{E_{max}}\right).$$

For an Yb:YAG laser with $\lambda_0 = 1030$ nm and the maximum X-ray photon energy $E_{max} = 12$ keV, we have $\gamma \approx 50$, i.e. $E_e = 25.5$ MeV. Figure 1 shows the X-ray photon energy as a function of the observation angle calculated by formula (3). This function defines the relation between the energy range of the X-ray photons generated by the source and the angle from which the optical system should 'capture' the radiation.

Since the electron beam has an angular spread in the focal region (the interaction domain), the function $E(\theta)$ is broadened. The broadening observed experimentally [5] amounts to 3%–5%. The domain marked in Fig. 1 corresponds to a band of width 3%. This signifies that it is inexpedient to use interference mirrors with spectral selectivity better than 3% as reflecting elements, since it will only lead to the loss of the useful signal.

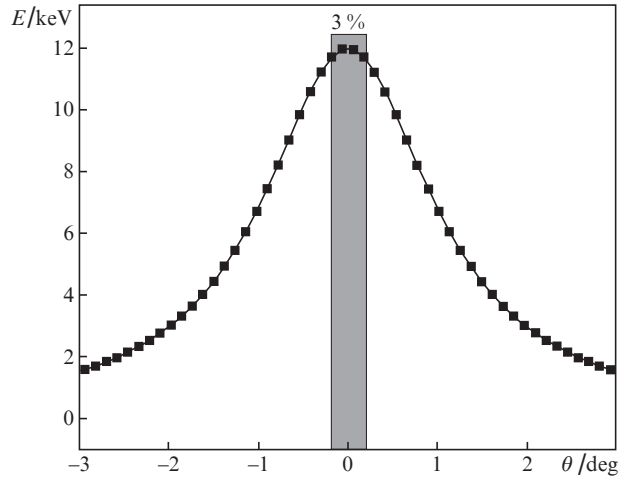

Figure 1. Energy of X-ray photons generated by the source based on the inverse Compton effect as a function of the observation angle for a laser wavelength $\lambda_0 = 1030$ nm.

3. Properties of Kirkpatrick–Baez setup as applied to the Compton source

The Kirkpatrick–Baez optical setup is intended for the two-dimensional focusing/collimation of X-ray radiation. In this case, the optics developers usually face the problem of collecting as many photons of the source as possible. The main features of the application of X-ray multilayer mirrors to the sources based on inverse Compton scattering are considered for the case when it is necessary to maximise the X-ray flux captured from the source in the photon energy range 10–12 keV. We also estimate the setup's efficiency for a 3% spectral capture bandwidth and consider the setups using total external reflection and multilayer interference mirrors (periodic multilayers and stack ones, i.e. stacks of several periodic mirrors deposited on top of each other [10]).

3.1. X-ray optical setup description

The X-ray optical Kirkpatrick–Baez setup is shown in Fig. 2. The distance of the first mirror from the X-ray source (500 mm) is determined by the thickness of the biological shield wall and the design of the two-mirror objective. The mirror length is chosen proceeding from the limiting capabilities of the facility for ion-beam mirror asphericisation and local error shape correction [11]. The distance from the object is determined by the requirement imposed on the focal spot, which should be equal to the source size (a one-fold magnification for the first mirror).

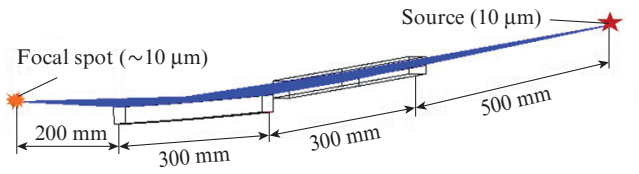

Figure 2. Design X-ray Kirkpatrick–Baez setup.

We analyse the geometry of radiation incidence on the mirrors in the Kirkpatrick–Baez setup (Fig. 3) so as to understand the major difference of the source under consideration from a monochromatic source with some angular width.

Let a beam with an angular width $2\Delta\theta$ and a wavelength λ be incident on a mirror of length L at a grazing angle θ_c (for the central ray). For the reflection of each ray incident on the mirror at a local angle θ_{loc} to be efficient, the Bragg equation must be fulfilled,

$$2d_{loc}\sin\theta_{loc} = \lambda, \quad (4)$$

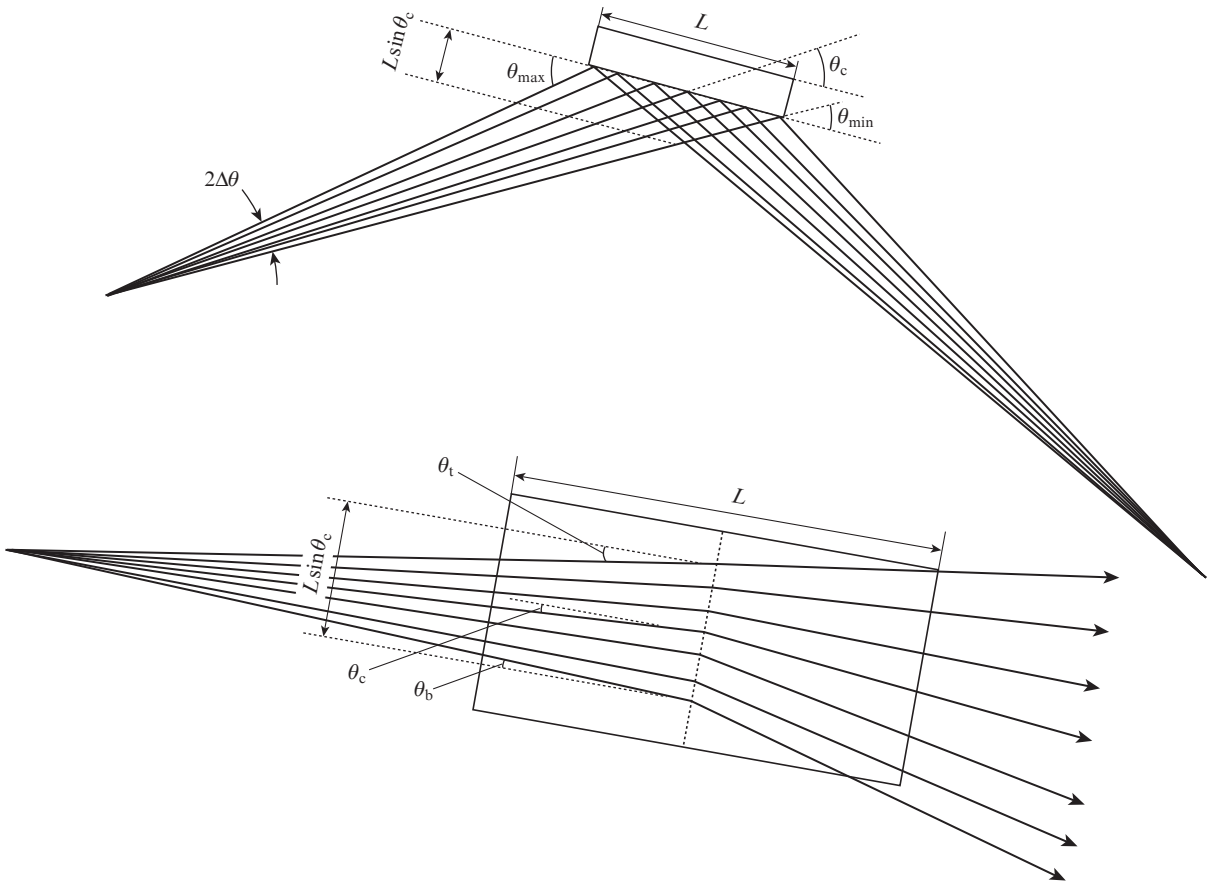

Figure 3. Diagram of ray paths (top and side views) in the reflection of a beam with an angular width $2\Delta\theta$ from a mirror of length L.

where d_{loc} is the local period of the multilayer coating. In the plane of the mirror, the grazing angles of the extreme rays of the beam are almost equal:

$$\theta_t \approx \theta_c \approx \theta_b, \tag{5}$$

and the local structure periods are equal. Therefore, to maximise the radiation collected from a monochromatic source, one must employ multilayer mirrors with a period varying in one direction along the surface (the so-called Göbel mirrors) [12].

The situation with the inverse Compton source is more complicated, since the beam contains photons with different wavelengths: $\lambda_{loc} = \lambda_{loc}(\theta_{loc})$. The local Bragg condition takes on the form

$$2d_{loc}\sin\theta_{loc} = \lambda_{loc}(\theta_{loc}). \tag{6}$$

It contains, obviously, a more significant change in the period of the multilayer mirror along the surface of the structure. However, this condition can be met, since the mirror length is hundreds of millimetres and it is easy to form a significant period gradient over this length. In the perpendicular direction, the grazing angle varies only slightly as before, but the wavelengths of radiation incident at the central and extreme points are different, $\lambda_t = \lambda_b \neq \lambda_c$, i.e. the structure period also varies in this direction. In this case, unlike the longitudinal direction, where the period varies in a length L of several hundred millimetres, in the transverse direction the period varies in a length $L\sin\theta_c$, which amounts to several millimetres. It is evident that there is no way of depositing a mirror with a period that varies several-fold in a length of several millimetres. This problem may be solved only with the use of broadband mirrors.

When a mirror intercepts a beam with an angular width $2\Delta\theta$ and the central grazing angle θ_c, it will receive rays in the angular range $\theta_c \pm \Delta\theta$, corresponding to the energy range from E_{min} to E_{max}. In this case, the value E_{max} is fixed and the minimal energy E_{min} is determined by the angle θ_c and the geometrical parameters of the setup (Table 1).

One can see from Table 1 that increasing the grazing angle increases the photon energy range captured by the mirror, i.e. improves the efficiency of the optical setup. The use of too small a grazing angle corresponding to total external reflection results in a significant increase in the geometrical dimensions of the system or in an energy loss. For a grazing angle $\theta_c \leqslant 0.6°$ we have $(E_{max} - E_{min})/E_{max} < 3\%$, which signifies the introduction of additional loss arising from the energy broadening of the Compton line. This value of the central grazing angle may be treated as the minimal possible one for the efficient use of the source. Increasing the radiation grazing angle is advantageous from the standpoint that the optical system captures the radiation in a broader energy range. However, the spectral bandwidth of interference mirrors becomes narrower with increasing working angle. This limits the efficiency of employment of multilayer mirrors in the sources based on the inverse Compton effect.

Table 1. Minimal X-ray photon energies E_{min}, captured by a mirror of length 300 mm and radiation collection angles $2\Delta\theta$ for different central radiation grazing angles θ_c.

θ_c /deg	E_{min} /keV	$(E_{max} - E_{min})/E_{max}$ (%)	$2\Delta\theta$ /deg
0.2	11.97	0.25	0.06
0.3	11.93	0.6	0.09
0.4	11.87	1.1	0.24
0.6	11.71	2.4	0.36
0.8	11.50	4.2	0.48
1.0	11.23	6.4	0.60
1.2	10.925	9.0	0.72
1.4	10.58	11.8	0.84
1.6	10.21	14.9	0.96

3.2. Optimisation of X-ray mirror parameters

In the optimisation of X-ray mirror parameters, we assume that the quantum source efficiency $I(\theta)$, which defines the number of photons emitted in a unit solid angle per second, is approximately described [4] (Fig. 4) by the Gaussian function of the form

$$I(\theta) = I_0 \exp\left[-\frac{(\theta - \theta_c)^2}{2\sigma^2}\right], \tag{7}$$

where $\sigma = 8.5$ mrad and $I_0 = 12 \times 10^8$ photon s^{-1} mrag^{-2} (the total flux is 2×10^{12} photon s^{-1}). According to formula (1), the X-ray photon energy and the angle θ are unambiguously related; the expression for the total energy of the radiation source in the angular range $\Delta\theta$ is represented in the form

$$E_{source} = \int_0^{\Delta\theta} I(\theta) E(\theta) 2\pi\theta \mathrm{d}\theta \tag{8}$$

(the integrand is the product of the number of photons and the energy of a single photon). In expression (8) we pass to integration with respect to dE in view of formula (3) to obtain

$$E_{source} = \frac{4\pi hc}{\lambda_0} I_0 \int_{E_{min}}^{E_{max}} I(E) \frac{\mathrm{d}E}{E},$$

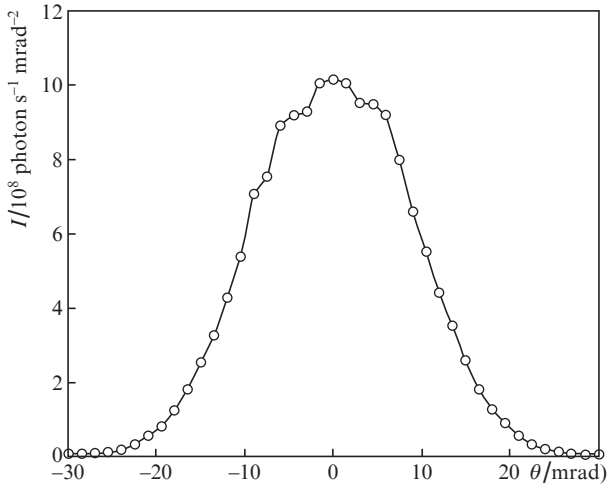

Figure 4. Dependence of X-ray radiation intensity on the observation angle for an energy of ~12 keV for a source based on the inverse Compton effect [4].

or (as a function of the maximal energy)

$$E_{source} = \frac{4\pi hc}{\lambda_0} I_0 \exp\left(\frac{2hc}{\sigma^2 \lambda_0 E_{max}}\right) \times \int_{E_{min}}^{E_{max}} \exp\left(-\frac{2hc}{\sigma^2 \lambda_0 E}\right) \frac{1}{E} \mathrm{d}E. \tag{9}$$

For $\lambda_0 = 1030$ nm, $\sigma = 8.5$ mrad, an energy of ~10 keV, and $\exp[-2hc/(\sigma^2\lambda_0 E)] \approx 1$, at the input of the X-ray optical setup we have

$$E_{source} = \frac{4\pi hc}{\lambda_0} I_0 \exp\left(\frac{2hc}{\sigma^2 \lambda_0 E_{max}}\right)\left(\frac{1}{E_{min}^2} - \frac{1}{E_{max}^2}\right). \tag{10}$$

Our task is to focus the radiation on a sample and, and doing this, to minimise the possible energy loss. Upon reflection from two X-ray mirrors at an angle θ_c, the signal takes on the form

$$E_{RR}(\theta_c) = \frac{4\pi hc}{\lambda_0} I_0 \exp\left(\frac{2hc}{\sigma^2 \lambda_0 E_{max}}\right) \int_{E_{min}(\theta_c)}^{E_{max}} R^2(\theta_c, E) \times \exp\left(-\frac{2hc}{\sigma^2 \lambda_0 E}\right) \frac{1}{E} \mathrm{d}E, \tag{11}$$

where the X-ray mirror reflection coefficient $R(\theta_c, E)$ depends on the incident photon energy E and the angle θ_c, which also defines the photon energy range captured by the mirror for a Compton source. Considering that the exponent in the integrand is close to unity, the optical efficiency of the system consisting of two X-ray mirrors may be represented as

$$\varepsilon_2(\theta_c) = \frac{E_{RR}(\theta_c)}{E_{source}} = \frac{\int_{E_{min}(\theta_c)}^{E_{max}} R^2(\theta_c, E) E^{-1} \mathrm{d}E}{1/E_{min}^2 - 1/E_{max}^2}. \tag{12}$$

Therefore, the task of maximising the integral setup efficiency is to find the X-ray multilayer mirror parameters that maximise integral (11) for a fixed grazing angle θ_c and then to find the optimal angle θ_c.

When E^{-1} in the integrand in expression (12) is replaced with a constant, this entails an error of ~10% in the determination of the efficiency, and the problem, in a sense, is reduced to the known one: the search for a mirror with the highest integral reflection coefficient with the inclusion of double reflection. It is well known that a large integral reflection coefficient can be obtained using aperiodic mirrors [13]. However, from the point of view of manufacturing and certification of broadband mirrors, it is more efficient to use not classical aperiodic mirrors, but stack structures [14, 15], because the labour expenditures for depositing them are an order of magnitude lower. These mirrors permit broadening the reflection band, but their peak reflectivity is evidently lower than that for a periodic mirror. For a multimirror setup (number of mirrors: m) the integrand contains R^m and not R^2. Therefore, it is *a priori* not clear how efficient this approach will be: each mirror captures radiation in a broader energy band, but the

effect of reflectivity lowering will be progressively stronger with increase in the number of mirrors m.

For a reflective coating of the total external reflection mirror we considered platinum Pt, because this heavy material provides a large critical angle and, in the case of multilayer mirrors, the Pt/C pair provides a high reflectivity in the 10–12 keV energy range. Furthermore, according to Ref. [13] the Pt/C mirrors, unlike, for instance, W/C mirrors, which also provide a high reflectivity, necessitate a smaller number of layers. This is of importance in the optimisation of the stack structure, since it entails the possibility of using a smaller number of stacks and therefore simplifies the technological process significantly. For an energy of about 10–12 keV ($\lambda \approx 0.10$–0.12 nm) and a grazing angle close to 1°, according to the Bragg equation we obtain periods of about 2–5 nm for Pt/C mirrors. For our calculations we assumed an interlayer roughness of ~ 0.3 nm. The densities of all materials were taken to be equal to the tabular ones.

Expression (12) was optimised using the Multifitting code [16], which permits calculating X-ray reflectivities of arbitrary layered structures as well as solving optimisation problems: to maximise a given integral or minimise the difference of the calculated curve from a given one. For a thick Pt film we calculated the reflectivities and efficiencies (12) for grazing angles of 0.2°–0.4° in the total external reflection domain. The reflectivity curves are plotted in Fig. 5 and the calculated efficiencies are collected in Table 2.

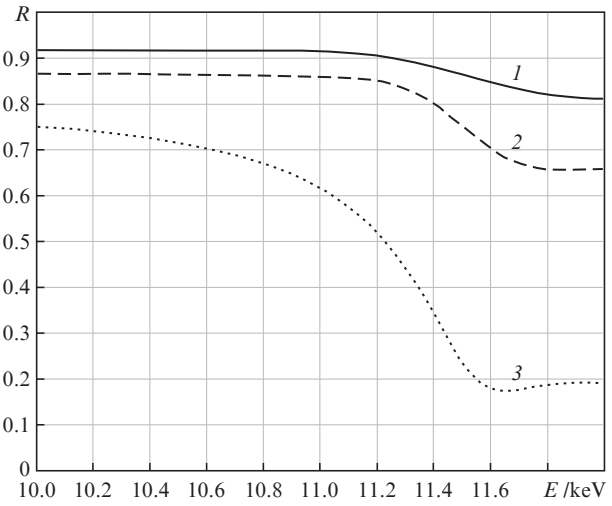

Figure 5. Reflectivity curves of the total external reflection Pt mirror for grazing angles θ_c = (*1*) 0.2°, (*2*) 0.3°, and (*3*) 0.4°.

In the optimisation of the parameters of periodic Pt/C mirrors, their thickness was taken to exceed the radiation extinction depth in the material (the bilayer number $N = 80$). Expression (12) was optimised by varying the period d and β fraction of the scattering Pt layer in the period. The resultant data are given in Fig. 6 and Table 2. For $\theta_c = 0.8°$, the spectral width of the Pt/C-mirror reflectivity curve is $\sim 3\%$, i.e. all X-ray photons with an energy of 12 keV are captured. In this case, the single-reflection coefficient of the mirror is 83.3%, and for a double reflection we obtain an efficiency of 69% for a spectral bandpass of 3%.

To broaden the spectral reflectivity curve, we optimised the parameters of the stack structures consisting of two periodic Pt/C mirrors, each being characterised by the combination of parameters $\{d_i, \beta_i, N_i\}$ (the subscript i numbers the stacks from the surface). For the upper mirror, the values of d_1, β_1, and N_1 were varied over wide ranges. For the lower mirror on the substrate, the thickness was taken to be very large ($N_2 = 100$) and parameters d_2 and β_2 were optimised. The broadened spectral reflectivity curves for one stack mirror are plotted in Fig. 7 and the double-reflection efficiencies are given in Table 2. The case of a three-stack mirror was considered for an angle $\theta_c = 0.8°$ (this angle corresponds to the highest efficiency calculated for periodic mirrors).

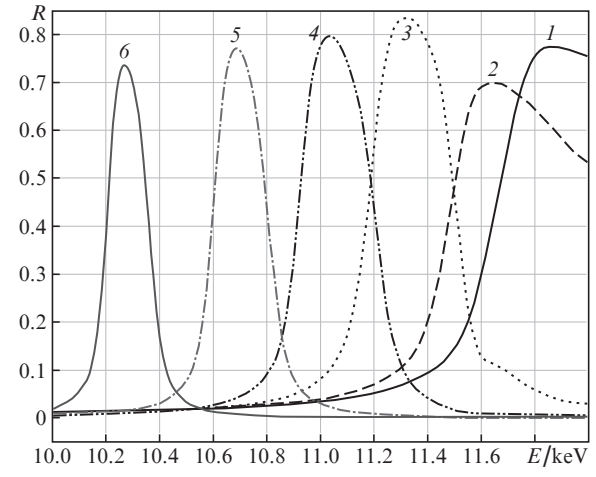

Figure 6. Reflectivity curves of periodic X-ray Pt/C mirrors optimised for maximum efficiency at grazing angles θ_c = (*1*) 0.6°, (*2*) 0.8°, (*3*) 1.0°, (*4*) 1.2°, (*5*) 1.4°, and (*6*) 1.6°.

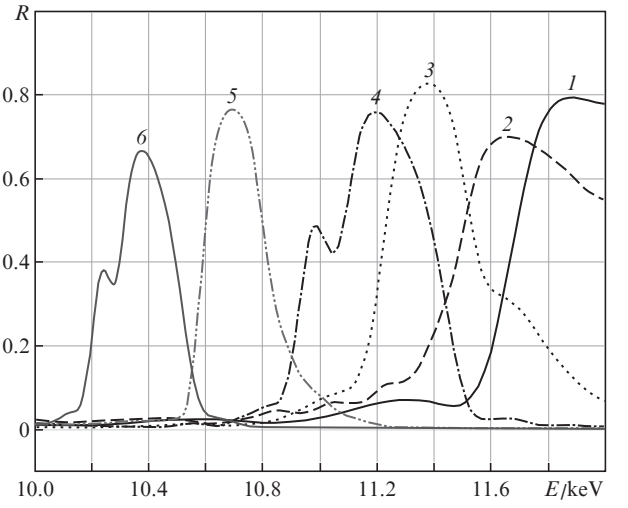

Figure 7. Reflectivity curves of stack X-ray Pt/C mirrors optimised for maximum efficiency at grazing angles θ_c = (*1*) 0.6°, (*2*) 0.8°, (*3*) 1.0°, (*4*) 1.2°, (*5*) 1.4°, and (*6*) 1.6°.

Our analysis makes it possible to determine the optimal, from the viewpoint of saving the source radiation power, grazing angle in the Kirkpatrick–Baez setup. Figure 8 shows the efficiency of the two-mirror optical setup calculated as a function of the grazing angle. One can see that the efficiency of total external reflection mirrors is an order of magnitude

Table 2. Kirkpatrick–Baez setup efficiencies ε_2 calculated by formula (12) for different central angles θ_c of grazing incidence for optimised mirrors of different types (for stack structures, the numbering begins from the surface).

θ_c /deg	Pt mirror	Periodic Pt/C mirror		Stack Pt/C mirror	
	ε_2 (%)	ε_2 (%)	Parameters	ε_2 (%)	Parameters
0.2	1.0	–	–	–	–
0.3	1.5	–	–	–	–
0.4	0.2	4.7	d = 80.6 Å, β = 0.1	–	–
0.6	–	9.0	d =52.4 Å, β = 0.20	9.55	N_1 = 14, d_1 = 51.9 Å, β_1 = 0.16 N_2 = 100, d_2 = 52.6 Å, β_2 = 0.20
0.8	–	11.0	d = 39.5 Å, β = 0.32	11.8	N_1 = 2, d_1 = 37.8 Å, β_1 = 0.20 N_2 = 15, d_2 = 39.0 Å, β_2 = 0.27 N_3 = 100, d_3 = 39.7 Å, β_3 = 0.34
1.0	–	9.5	d = 32.4 Å, β = 0.37	10.0	N_1 = 20, d_1 = 31.9 Å, β_1 = 0.37 N_2 = 100, d_2 = 32.4 Å, β_2 = 0.38
1.2	–	7.6	d = 27.6 Å, β = 0.41	9.2	N_1 = 44, d_1 = 26.9 Å, β_1 = 0.35 N_2 = 100, d_2 = 27.6 Å, β_2 = 0.38
1.4	–	5.2	d = 24.3 Å, β = 0.40	5.8	N_1 = 21, d_1 = 24.0 Å, β_1 = 0.38 N_2 = 100, d_2 = 24.3 Å, β_2 = 0.42
1.6	–	3.7	d = 22.0 Å, β = 0.40	4.3	N_1 = 66, d_1 = 21.7 Å, β_1 = 0.37 N_2 = 100, d_2 = 22.0 Å, β_2 = 0.40

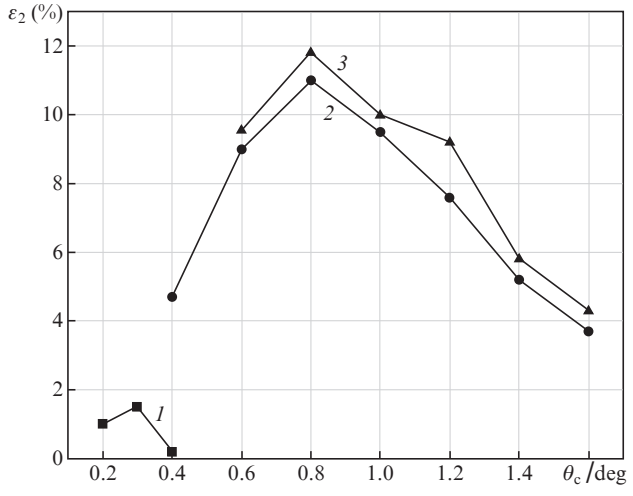

Figure 8. Efficiency of the optical setup for source radiation collection as a function of the grazing angle for (*1*) the total external reflection Pt mirror, (*2*) optimised periodic Pt/C mirrors, and (*3*) optimised stack Pt/C mirrors.

lower than that of interference mirrors due to the narrow energy collection range at grazing incidence angles. As the grazing angle increases, the radiation energy range captured by the optical setup becomes broader, but the Bragg condition causes the reflection peak to shift to the lower energy domain, and the spectral width of the reflectivity curve is narrower at larger angles. The competition of these two effects determines the existence of the efficiency peak near an angle $\theta_c = 0.8°$.

4. Conclusions

We have shown that the principles of multilayer mirror optimisation for the sources based on the inverse Compton effect are different from those for sources of other types. The main efficiency limitation for these mirrors is the dependence of the wavelength on the observation angle. Efficient radiation collection calls for the use of broadband mirrors.

The efficiency of total external reflection mirrors is an order of magnitude lower than that of multilayer mirrors. Stack interference mirrors offer a small advantage over the periodic ones. This advantage becomes greater with increase in photon energy and in the case of a single reflection setup. The overall efficiency of the Kirkpatrick–Baez setup for a photon energy range of 10–12 keV amounts to 12%; in a spectral bandwidth of 3% the efficiency is 69%.

Acknowledgements. This work was performed within the framework of State Assignment No. 0035-2014-0204 under support from the Presidium of the RAS (Fundamental Research Programme I.1 'Extreme Light Fields and Their Interaction with Matter' No. 0035-2018-0018). The modification of the Multifitting code for the solution of optimisation problems in the class of stack structures was supported by the Russian Foundation for Basic Research (Grant No. 18-32-00173).

References

1. Mills D., Padmore H., Lessner E. https://www.osti.gov/biblio/1287448.
2. Huang Z., Ruth R.D. *Phys. Rev. Lett.*, **80** (5), 976 (1998).
3. Bech M., Bunk O., David C., Ruth R., Rifkin J., Loewen R., Feidenhans'l R., Pfeiffer F. *J. Synchrotron Radiat.*, **16** (1), 43 (2009).
4. Graves W.S., Bessuille J., Brown P., Carbajo S., Dolgashev V., Hong K.-H., Ihloff E., Khaykovich B., Lin H., Murari K., Nanni E.A., Resta G., Tantawi S., Zapata L.E., Kärtner F.X., Moncton D.E. *Phys. Rev. Spec. Top. Accel. Beams*, **17**, 120701 (2014).
5. Hornberger B., Kasahara J., Gifford M., Ruth R., Loewen R. *Proc. SPIE*, **11110**, 1111003 (2019); DOI: 10.1117/12.2527356.
6. Eggl E., Schleede S., Bech M., Achterhold K., Grandl S., Sztrókay A., Hellerhoff K., Mayr D., Loewen R., Ruth R.D., Reiser M.F., Pfeiffer F. *Eur. Phys. Lett.*, **116** (6), 68003 (2016).
7. Eggl E., Mechlem K., Braig E., Kulpe S., Dierolf M., Günther B., Achterhold K., Herzen J., Gleich B., Rummeny E., Noël P.B., Pfeiffer F., Muenzel D. *Sci. Rep.*, **7**, 42211 (2017).
8. Snigirev A., Kohn V., Snigireva I., Lengeler B. *Nature*, **384** (6604), 49 (1996); DOI: 10.1038/384049a0.
9. Kirkpatrick P., Baez A.V. *J. Opt. Soc. Am.*, **38**, 766 (1948).
10. Kuhlmann T., Yulin S., Feigl T., Kaiser N., Bernitzki H., Lauth H. *Proc. SPIE*, **4688**, 509 (2002).

11. Chkhalo N.I., Kaskov I.A., Malyshev I.V., Mikhaylenko M.S., Pestov A.E., Polkovnikov V.N., Salashchenko N.N., Toropov M.N., Zabrodin I.G. *Precis. Eng.*, **48**, 338 (2017).
12. Göbel H. *J. Phys. D: Appl. Phys.*, **28**, A270 (1995).
13. Kozhevnikov I.V., Bukreeva I.N., Ziegler E. *Nucl. Instrum. Methods Phys. Res.*, *Sect. A*, **460** (2-3), 424 (2001).
14. Barysheva M.M., Garakhin S.A., Zuev S.Yu., Polkovnikov V.N., Salashchenko N.N., Svechnikov M.V., Chkhalo N.I., Yulin S. *Quantum Electron.*, **49** (4), 380 (2019) [*Kvantovaya Elektron.*, **49** (4), 380 (2019)].
15. Barysheva M.M., Garakhin S.A., Zuev S.Yu., Polkovnikov V.N., Salashchenko N.N., Svechnikov M.V., Smertin R.M., Chkhalo N.I., Meltchakov E. *Tech. Phys*., **64**, 1673 (2019) [*Zh. Tekh. Fiz*., **89** 1763 (2019)].
16. http://xray-optics.ru/products/software-multifitting/.